

## PATTERN FORMATION IN AN ARRAY OF OSCILLATORS WITH ELECTRICAL AND CHEMICAL COUPLING\*

FATMA GUREL KAZANCI<sup>†</sup> AND BARD ERMENTROUT<sup>†‡</sup>

**Abstract.** Weak coupling theory is applied to a model for firing waves in the procerebral lobe of the slug. Inhibitory synapses and electrical synapses have different synchronizing properties. We show that, in concert, these two types of coupling can cause a bifurcation to a patterned state from synchrony which ultimately develops into traveling waves. Normal forms for the bifurcation are computed, and the results are compared to numerical simulations of the phase models.

**Key words.** electrical coupling, inhibition, oscillations, waves, synchrony

**AMS subject classifications.** 37G05, 92C20

**DOI.** 10.1137/060661041

**1. Introduction.** Networks of coupled neural oscillators exhibit a variety of activity patterns according to the properties of the coupling. There is clear experimental evidence for the existence of electrical and chemical synapses in neocortical inhibitory networks [11]. The effect of each type of coupling in isolation is well studied [4, 17, 19]. Depending on the nature of the neural oscillation, inhibition can be either synchronizing or desynchronizing [19, 12]. Electrical coupling between oscillators is established via gap junctions. In numerous computational and theoretical studies, it has been shown that electrical coupling can promote either synchrony or antisynchrony [18, 1, 4, 3], depending on the shape of the action potential and the nature of the oscillator. Recently, the combined effects of these couplings have been an area of theoretical interest [16, 13, 2, 17]. In these papers, both the inhibition and the gap junctions encouraged synchronization. Coupling is between pairs of oscillators or in all-to-all coupled networks.

In a recent paper [6], Ermentrout et al. explored a biophysical model for the olfactory lobe of the garden slug. Under resting conditions the slug lobe produces slow periodic traveling waves of electrical activity. The oscillations are generated by a class of inhibitory bursting neurons, which are coupled via gap junctions and chemical inhibitory synapses. Experimentally, the wave of activity is biased to move in one direction because of an intrinsic gradient in the frequency of the bursting cells. In the above paper, the authors developed and simulated a biophysical model for the waves with both inhibition and gap junctions. They found that even in the absence of a gradient in frequency, it was possible to generate waves in an otherwise homogeneous network. With large enough gap junction coupling (or small enough inhibition), the network synchronized. However, with weak electrical coupling the network becomes desynchronized, breaking into clusters of cells with different phase-lags. At intermediate coupling strengths, the network produces waves.

Our broad goal in this paper is to explore what happens in spatially distributed

---

\*Received by the editors May 26, 2006; accepted for publication (in revised form) November 7, 2006; published electronically February 9, 2007. The authors were supported by National Science Foundation grant DMS05135.

<http://www.siam.org/journals/siap/67-2/66104.html>

<sup>†</sup>Department of Mathematics, University of Pittsburgh, Pittsburgh, PA 15260 (fag4@pitt.edu, bard@math.pitt.edu).

<sup>‡</sup>Corresponding author.

networks when one form of coupling (here, gap junctions) encourages synchrony but the other form of coupling (chemical inhibition) encourages (at least pairwise) anti-phase (half cycle apart) locking. More specifically, we suppose that the synchronous coupling is local and the desynchronizing coupling is long range. Since electrical junctions require that membranes of the cells be in direct contact, we expect that gap junction coupling is spatially localized. In contrast, chemical inhibition might be expected to have longer range. In the slug brain model, the inhibition is global, in that each cell inhibited all the other cells in the network, while the gap junctions were only between nearest neighbors. We show below that inhibition is desynchronizing for the slug model and that gap junctions synchronize, so the slug model serves as an example of a spatially distributed network in which the two types of coupling work in opposition. Ermentrout and Kopell [10] explored the effects of one or two long range desynchronizing interactions between cells that were coupled with local synchronizing interactions. Various types of waves were found via direct analytic calculations which were possible due to the simple form of the coupling.

In this paper, we explore the bifurcation to patterns in a general network of oscillators in which there is long range desynchronizing coupling and short range synchronizing coupling. The strength of the former coupling is a parameter which when increased causes the synchronous state to lose stability. We determine the critical values for this parameter via linear stability analysis, and the direction of the bifurcation via a normal form calculation. To make the analysis possible and to avoid the confound of boundary effects, we forgo the linear chain and work on a circular domain. Numerical results of the chain produce similar behavior, but the analysis is considerably more difficult. The normal form calculation is made somewhat more difficult by the presence of a zero eigenvalue arising from translation invariance. Our method is to first reduce the biophysical model to a chain of phase-coupled oscillators on which we can apply the general theory. Thus, in the first section, after introducing the biophysical model, we compute the interaction functions under the assumption of weak coupling. We show that for this model, gap junctions are synchronizing, while chemical inhibition is desynchronizing. Next, we analyze the bifurcation of patterned states from synchrony in a continuum chain of phase-oscillators. We find a novel phase-locked state which is patterned but not a traveling wave. We numerically illustrate the transition to traveling waves as predicted in the reduced system and provide conditions for the stability of the traveling wave.

**2. The model and reduction.** Ermentrout et al. introduced a biophysical model for a network of bursting and nonbursting cells in the procerebral lobe of *Limax* [6]. The bursting cells oscillate at about 1 Hz and are responsible for the electrical wave observed in the lobe. The nonbursting cells fire only in the presence of extrinsic stimuli. Thus, since we are interested only in the genesis of the wave, we focus on the bursting cells. Each cell is an intrinsic oscillator, and, in the model, two types of synapses couple the oscillating neurons: chemical inhibition and electrical or gap junctions. The membrane potential for each bursting cell obeys the following equations:

$$C \frac{dV}{dt} = -I_L - I_K - I_{Ca} - I_{gap} - I_{syn},$$

where each term is a current due respectively to the leak, the potassium channels, the calcium channels, the gap junction coupling, and the synaptic inhibition. We used the parameters given in Appendix B. The gap junction coupling is over nearest neighbors

and depends on the voltage difference between the pre- and postsynaptic cells:

$$I_{gap} = g_{gap}(V_{post} - V_{pre}).$$

Here, “post” refers to the cell receiving the connection from the “pre” cell. The inhibition,  $I_{syn}$ , is global—every cell inhibits every other cell. Each synaptic interaction adds a current of the form

$$I_{syn} = g_{syn}s_{pre}(V_{post} - E_{syn}),$$

where  $E_{syn} = -78$  mV, and the synaptic conductance obeys an equation of the form

$$\frac{ds_{pre}}{dt} = \frac{0.1}{(1 + \exp(-(V_{pre} + 45)/5))} - \frac{s_{pre}}{100}.$$

Networks of coupled oscillators are generally difficult to analyze. However, the method of averaging has proven to be very useful for studying synchronization between oscillators [17]. That is, if we assume that the conductances  $g_{gap}$ ,  $g_{syn}$  are sufficiently small, it is possible to reduce a network of coupled oscillators to a system of phase models where each oscillator is represented by its scalar phase and interactions are through the differences in the phases [21, 15, 9]. Let  $V_i$  be the membrane potential of the  $i$ th cell and  $s_i$  be the synaptic component of the  $i$ th cell. If

$$-I_{syn,i} = -g_{syn} \sum_j w_{ij} s_j (V_i - E_{syn})$$

is the synaptic current into the  $i$ th cell and  $w_{ij}$  is the weight of the connection between cell  $i$  and  $j$ , which is taken to be  $1/N$ , where  $N$  is the number of oscillators, then with the weak coupling assumption, the phase interactions will take the form

$$(2.1) \quad -\bar{I}_{syn,i} = g_{syn} \sum_j w_{ij} H_{syn}(\theta_j - \theta_i),$$

where

$$H_{syn}(\phi) = \frac{1}{T} \int_0^T V^*(t) s(t + \phi) (E_{syn} - V(t)) dt.$$

$V^*(t)$  is the voltage component for the  $T$ -periodic solution to the adjoint equation for the stable limit cycle.  $V(t)$ ,  $s(t)$  are the voltage and synaptic components, respectively. For the gap junction coupling, we find

$$(2.2) \quad -\bar{I}_{gap,i} = g_{gap} \sum_j z_{ij} H_{gap}(\theta_j - \theta_i),$$

where

$$H_{gap}(\phi) = \frac{1}{T} \int_0^T V^*(t) (V(t + \phi) - V(t)) dt.$$

The weights,  $z_{ij}$ , satisfy  $z_{ij} = f(|i - j|)$ , where  $f$  is a decreasing function in its argument. The phase of each oscillator,  $\theta_i$ , obeys the reduced dynamics

$$\theta'_i = 1 - \bar{I}_{syn,i} - \bar{I}_{gap,i},$$

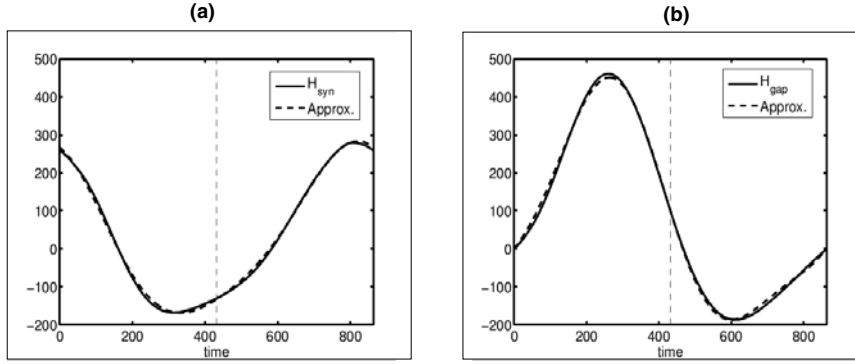


FIG. 2.1. Coupling functions are computed using XPPAUT. Approximations are estimated from the Fourier expansion. (a) shows  $H_{syn}$  and its approximation, and (b) shows  $H_{gap}$  and its approximation. The functions are plotted over a period of the oscillations, and the dashed line marks the half period.

where the two currents are given by (2.1) and (2.2). The phase of each oscillator maps directly onto the potential (or other variable) of each bursting cell once the zero phase is chosen. A standard choice of zero phase is the peak of the membrane potential.

Figure 2.1 shows both  $H_{syn}$  and  $H_{gap}$  for the Limax model evaluated numerically using XPPAUT [5], along with their approximations using the 0, 1, 2 order terms of the Fourier expansion. The Fourier approximations of these functions are used in bifurcation calculations in section 3, the stability arguments in section 4, and the numerical simulations of the phase model in section 5. Their values are given in Appendix B. Note that  $H_{syn}(0) \neq 0$ ,  $H_{gap} = 0$ ,  $H'_{syn}(0) < 0$ , and  $H'_{gap}(0) > 0$ .

To interpret the meaning of these inequalities, consider a pair of identical cells:

$$\begin{aligned} \theta'_1 &= 1 + g_{syn}H_{syn}(\theta_2 - \theta_1) + g_{gap}H_{gap}(\theta_2 - \theta_1), \\ \theta'_2 &= 1 + g_{syn}H_{syn}(\theta_1 - \theta_2) + g_{gap}H_{gap}(\theta_1 - \theta_2). \end{aligned}$$

Let  $\phi = \theta_2 - \theta_1$ . Then

$$\phi' = g_{syn}[H_{syn}(-\phi) - H_{syn}(\phi)] + g_{gap}[H_{gap}(-\phi) - H_{gap}(\phi)] \equiv F(\phi).$$

Clearly,  $F(0) = 0$ , so synchrony,  $\theta_2 = \theta_1$ , is a solution. Synchrony is stable if  $F'(0) < 0$  or

$$g_{syn}H'_{syn}(0) + g_{gap}H'_{gap}(0) > 0.$$

Since the conductances,  $g_{syn}$ ,  $g_{gap}$  are nonnegative and  $H'_{syn}(0) < 0$ ,  $H'_{gap}(0) > 0$ , synchrony is stable if the gap junctions dominate. Since  $F(\phi)$  is an odd  $T$ -periodic function,  $F(T/2) = 0$ . This *antiphase* solution will be stable for the coupled pair if  $F'(T/2) < 0$  or, equivalently,

$$g_{syn}H'_{syn}(T/2) + g_{gap}H'_{gap}(T/2) > 0.$$

As seen in Figure 2.1 by the dashed vertical lines at  $T/2$ , antiphase is stable for synaptic and unstable for gap junction coupling. In the models considered by Lewis and Rinzel, both synaptic and electrical coupling encourage stable synchrony [16]. Thus, the interaction of networks will lead to synchronous behavior. In contrast, for

the intrinsic dynamics in the Limax model, electrical coupling encourages synchrony, but synaptic inhibition opposes it. Our goal in the rest of this paper is to explore the consequences of these differences in a one-dimensional spatially organized array of  $N$  oscillators.

**2.1. The spatial equations.** We introduce a discrete model where we have all-to-all synaptic coupling and local gap junction coupling. The equations can be written down as

$$(2.3) \quad \frac{d\theta_j}{dt} = \omega + \frac{g_{syn}}{N} \sum_{k=1}^N H_{syn}(\theta_k - \theta_j) + g_{gap} \sum_{l=-m}^m J_l H_{gap}(\theta_{j+l} - \theta_j), \quad j = 1, \dots, N,$$

where  $\theta_j$  represents the phase of oscillator  $j$ ,  $\omega$  is the intrinsic frequency for all the oscillators,  $g_{syn}$  is the synaptic coupling strength,  $g_{gap}$  is the strength of electrical coupling, and  $H_{syn}$ ,  $H_{gap}$  are the functions describing synaptic and gap junction coupling, respectively. We note that the key point in the weak coupling assumption is that the effects of different types of coupling are linear and additive. Thus, only the ratio of  $g_{syn}$  and  $g_{gap}$  in the phase model matter. The oscillators are arranged in a ring to avoid boundary effects. W.l.o.g., we assume that the ring has length  $2\pi$ . The factor  $\frac{1}{N}$  in front of the synaptic coupling contribution guarantees that the model also works when we allow  $N \rightarrow \infty$ . The weights  $J_l$  are taken to be nonnegative, and we assume that  $J_{-l} = J_l$ .  $m$  represents the scope of gap junction coupling. We also note that  $m \ll N$ , since we assume that gap junction coupling is local. Henceforth, we assume that the period of the oscillators (and thus of the coupling functions) is  $2\pi$ . The function  $H_{syn}$  favors the antiphase state for pairwise interactions so that  $\pi$  is a stable fixed point for a pair of oscillators coupled with only synaptic coupling. The function  $H_{gap}$  favors the in-phase state for pairwise interactions so that 0 is a stable fixed point for a pair of oscillators coupled with only gap junction coupling. This is equivalent to saying the following:

A1.  $H'_{syn}(0) < 0$ .

A2.  $H'_{gap}(0) > 0$ .

For simplicity, we also need the following:

A3.  $H_{syn}(0) = 0$ .

A4.  $H_{gap}(0) = 0$ .

Note that A4 holds automatically for gap junctions, since a cell cannot be coupled to itself via gap junctions. If  $H_{syn}(0) = \kappa \neq 0$ , then let  $\theta_j = \hat{\theta}_j + (\omega + g_{syn}\kappa)t$ . We write

$$\frac{d\hat{\theta}_j}{dt} = \frac{g_{syn}}{N} \sum_{k=1}^N \hat{H}_{syn}(\hat{\theta}_k - \hat{\theta}_j) + g_{gap} \sum_{l=-m}^m J_l H_{gap}(\hat{\theta}_{j+l} - \hat{\theta}_j), \quad j = 1, \dots, N,$$

where  $\hat{H}_{syn}(\phi) = H_{syn}(\phi) - \kappa$ . We can see that  $\hat{H}_{syn}(0) = 0$ , so w.l.o.g., we assume  $H_{syn}(0) = 0$ .

We also make a normalization assumption on  $J_l$  by taking the following:

A5\*.  $\sum_{l=-m}^m J_l = 1$ .

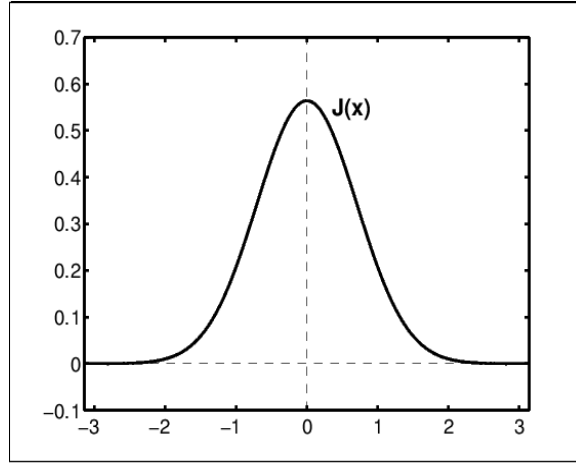


FIG. 2.2. A plot of  $J(x)$  where the sum was taken over  $n = -2, -1, 0, 1, 2$ .

For the purposes of calculations, it is much easier to work with the continuum analogue of (2.3), so our analysis will be on a continuum version of the network. Hence, from now on, we study this model

$$(2.4) \quad \begin{aligned} \frac{\partial \theta}{\partial t} = & \omega + \frac{g_{syn}}{2\pi} \int_0^{2\pi} H_{syn}(\theta(y) - \theta(x)) dy \\ & + g_{gap} \int_0^{2\pi} J(x - y) H_{gap}(\theta(y) - \theta(x)) dy, \end{aligned}$$

where analogous assumptions are made as for the discrete model. We remark that the continuum model can be derived from the discrete model in the limit as  $N \rightarrow \infty$  with a suitable normalization assumption on the function  $J_\ell$ . One difference is that the discrete model,  $\theta_j$ , was a function of time and the discrete index  $j$ , whereas it is now a function of time and space. We assume that  $J(x)$  is a nonnegative, symmetric kernel around 0 and that the normalization condition is

$$A5. \int_0^{2\pi} J(y) dy = 1.$$

In our numerical simulations, we assumed  $J(x) = \sum_{n=-\infty}^{\infty} \exp(-(x + 2\pi n)^2) / \sqrt{\pi}$ . (See Figure 2.2.)

**3. Linear stability analysis for synchronous solution.** We want to study the spatial interactions between synchronizing and antisynchronizing influences. We start with the synchronous state and study its stability. The synchronous state is where all of the oscillators have the same phase. Note that if we assume heterogeneity in the intrinsic frequencies, synchrony is not a solution to the system. If we have homogeneity,  $\theta(x, t) = \Omega t$  is a solution to (2.4), where  $\Omega = \omega + g_{syn} H_{syn}(0)$  represents the frequency of the network. To determine the stability of synchrony, we let  $\theta(x, t) = \Omega t + \psi(x, t)$  and write

$$(3.1) \quad \begin{aligned} \frac{\partial \psi}{\partial t} = & \frac{g_{syn}}{2\pi} \int_0^{2\pi} H'_{syn}(0) [\psi(y) - \psi(x)] dy \\ & + g_{gap} \int_0^{2\pi} J(x - y) H'_{gap}(0) [\psi(y) - \psi(x)] dy + O(|\psi|^2). \end{aligned}$$

If we keep only the linear terms above, we can see that  $\psi(x, t) = e^{inx} e^{\lambda_n t}$  solves (3.1) with the appropriate choice of  $\lambda_n$ . Let  $I_n = \int_0^{2\pi} J(s) e^{-ins} ds$ , and substitute  $\psi(x, t)$  into (3.1) to get

$$(3.2) \quad \lambda_n = -g_{syn} H'_{syn}(0) + g_{gap} H'_{gap}(0) [I_n - 1]$$

for  $n \neq 0$ . For  $n = 0$ ,  $\lambda_0 = 0$ . We choose  $J(x)$  so that we have  $I_1 \geq 1$  and  $I_1 > I_2 > \dots > I_n > I_{n+1} > \dots$ . This means that the first Fourier mode dominates. The Gaussian kernel shown in Figure 2.2 satisfies this criterion, as does, for example, the periodic version of an exponential kernel,  $\exp(-|x|)$ . With this assumption, it is easy to see that the first eigenvalue to cross over to positive values would be  $\lambda_1$ . We call  $n = 1$  the most unstable node. To find the critical value of  $g_{syn}$ , we solve for  $\lambda_1 = 0$ , which gives us

$$(3.3) \quad g_{syn}^* = \frac{g_{gap} H'_{gap}(0) [I_1 - 1]}{H'_{syn}(0)}.$$

Here \* is used to denote the value of  $g_{syn}$  at the bifurcation point. To study the stability of the bifurcating solutions we need to find the normal form for the bifurcation. We prove the following theorem.

**THEOREM 3.1.** *The system (2.4) with the assumptions A1–A5 has a pitchfork bifurcation at  $g_{syn}^*$ , and the corresponding normal form is*

$$0 = \zeta z^2 \bar{z} + \eta z.$$

The coefficients  $\zeta$  and  $\eta$  are

$$\begin{aligned} \zeta &= 12B_{1,3} - 3B_{2,3} - 9B_{0,3} + 2C B_{0,2} - 2CB_{2,2}, \\ \eta &= -g_2\alpha_1, \end{aligned}$$

where

$$\begin{aligned} B_{n,j} &= \int_0^{2\pi} A_j(y') e^{iny'} dy', \\ A_j(x) &= \frac{g_{syn}^*}{2\pi} \alpha_j + g_{gap} \beta_j J(x), \\ C &= \frac{2B_{1,2} - B_{2,2} - B_{0,2}}{B_{2,1} - B_{0,1}}, \end{aligned}$$

with  $\alpha_j = \frac{H_{syn}^j(0)}{j!}$  and  $\beta_j = \frac{H_{gap}^j(0)}{j!}$  for  $j = 1, 2, \dots$ . Here  $f^j(x_0)$  represents the  $i$ th derivative at  $x_0$  for  $f = H_{syn}, H_{gap}$ .

*Proof.* We use a perturbation expansion for the solution  $\psi$  and  $g_{syn}$  as

$$(3.4) \quad \theta(x, t) = \Omega(\epsilon) t + \hat{\psi}(x, \epsilon),$$

where

$$\begin{aligned} \Omega(\epsilon) &= \epsilon \Omega_1 + \epsilon^2 \Omega_2 + \epsilon^3 \Omega_3 + \dots, \\ \hat{\psi}(x, \epsilon) &= \epsilon \psi_1(x) + \epsilon^2 \psi_2(x) + \epsilon^3 \psi_3(x) + \dots, \end{aligned}$$

and

$$g_{syn} = g_{syn}^* + \epsilon g_1 + \epsilon^2 g_2.$$

We define a linear operator  $\mathcal{L}$  as follows:

$$\begin{aligned} \mathcal{L}\psi &= \frac{g_{syn}^*}{2\pi} \int_0^{2\pi} H'_{syn}(0)[\hat{\psi}(y, \epsilon) - \hat{\psi}(x, \epsilon)] dy \\ &\quad + g_{gap} \int_0^{2\pi} J(x-y)H'_{gap}(0)[\hat{\psi}(y, \epsilon) - \hat{\psi}(x, \epsilon)] dy \\ &= \frac{g_{syn}^*}{2\pi} \int_0^{2\pi} H'_{syn}(0)[\hat{\psi}(x-y', \epsilon) - \hat{\psi}(x, \epsilon)] dy' \\ (3.5) \quad &\quad + g_{gap} \int_0^{2\pi} J(y')H'_{gap}(0)[\hat{\psi}(x-y', \epsilon) - \hat{\psi}(x, \epsilon)] dy' \end{aligned}$$

with the substitution  $y' = x - y$ . Note that  $e^{\pm ix}$ ,  $\mathbf{1}$  are in the null space of  $\mathcal{L}$  and that  $\mathcal{L}$  is self-adjoint. (Here, we use  $\mathbf{1}$  to denote the constant function which is 1 for all  $x$ .) We need to find the Taylor expansions of  $H_{syn}$  and  $H_{gap}$  around 0 for the full system

$$\begin{aligned} H_{syn}(x) &= H_{syn}(0) + H'_{syn}(0) x + \frac{H''_{syn}(0)}{2} x^2 + \frac{H'''_{syn}(0)}{6} x^3 + \dots \\ &= \alpha_1 x + \alpha_2 x^2 + \alpha_3 x^3 + \dots, \\ H_{gap}(x) &= H_{gap}(0) + H'_{gap}(0) x + \frac{H''_{gap}(0)}{2} x^2 + \frac{H'''_{gap}(0)}{6} x^3 + \dots \\ &= \beta_1 x + \beta_2 x^2 + \beta_3 x^3 + \dots. \end{aligned}$$

Substituting  $\theta$  in the form given in (3.4) into (2.4),

$$\begin{aligned} \Omega(\epsilon) &= \frac{(g_{syn}^* + \epsilon g_1 + \epsilon^2 g_2)}{2\pi} \int_0^{2\pi} \alpha_1 [\hat{\psi}(x-y', \epsilon) - \hat{\psi}(x, \epsilon)] dy' \\ &\quad + \frac{(g_{syn}^* + \epsilon g_1 + \epsilon^2 g_2)}{2\pi} \int_0^{2\pi} \alpha_2 [\hat{\psi}(x-y', \epsilon) - \hat{\psi}(x, \epsilon)]^2 dy' \\ &\quad + \frac{(g_{syn}^* + \epsilon g_1 + \epsilon^2 g_2)}{2\pi} \int_0^{2\pi} \alpha_3 [\hat{\psi}(x-y', \epsilon) - \hat{\psi}(x, \epsilon)]^3 dy' \\ &\quad + g_{gap} \int_0^{2\pi} J(y') \beta_1 [\hat{\psi}(x-y', \epsilon) - \hat{\psi}(x, \epsilon)] dy' \\ &\quad + g_{gap} \int_0^{2\pi} J(y') \beta_2 [\hat{\psi}(x-y', \epsilon) - \hat{\psi}(x, \epsilon)]^2 dy' \\ (3.6) \quad &\quad + g_{gap} \int_0^{2\pi} J(y') \beta_3 [\hat{\psi}(x-y', \epsilon) - \hat{\psi}(x, \epsilon)]^3 dy' + O(|\hat{\psi}|^4). \end{aligned}$$

Let  $A_j(x) = \frac{g_{syn}^*}{2\pi} \alpha_j + g_{gap} \beta_j J(x)$  for  $j = 1, 2, 3$  and  $Q(x) = \int_0^{2\pi} [\alpha_1(\hat{\psi}(x-y', \epsilon) - \hat{\psi}(x, \epsilon)) + \alpha_2(\hat{\psi}(x-y', \epsilon) - \hat{\psi}(x, \epsilon))^2 + \alpha_3(\hat{\psi}(x-y', \epsilon) - \hat{\psi}(x, \epsilon))^3] dy'$ , which lets us to

rewrite (3.6) as

$$\begin{aligned}
 \Omega(\epsilon) &= \int_0^{2\pi} A_1(y') [\hat{\psi}(x - y', \epsilon) - \hat{\psi}(x, \epsilon)] dy' \\
 &\quad + \int_0^{2\pi} A_2(y') [\hat{\psi}(x - y', \epsilon) - \hat{\psi}(x, \epsilon)]^2 dy' \\
 &\quad + \int_0^{2\pi} A_3(y') [\hat{\psi}(x - y', \epsilon) - \hat{\psi}(x, \epsilon)]^3 dy' \\
 (3.7) \quad &\quad + \epsilon \frac{g_1}{2\pi} Q(x) + \epsilon^2 \frac{g_2}{2\pi} Q(x) + O(|\hat{\psi}|^4).
 \end{aligned}$$

We match the coefficients of powers of  $\epsilon$  terms from both sides of (3.7). This allows us to compute the coefficients for the normal form. The rest of the calculations are given in the appendix. The normal form for the bifurcation is

$$0 = \zeta z^2 \bar{z} + \eta z,$$

where  $\zeta = 12B_{1,3} - 3B_{2,3} - 9B_{0,3} + 2CB_{0,2} - 2CB_{2,2} - 2CB_{2,2}$  and  $\eta = -g_2\alpha_1$ . Note that  $\eta$  is positive since  $\alpha_1 < 0$  from our assumptions. Thus, depending on the sign of  $\zeta$ , we can determine the stability of the new solutions.  $\square$

In our case, we compute  $\zeta = -210.09$  and  $\eta = 105g_2$ , which tells us that we have a supercritical pitchfork bifurcation. The new solution bifurcating from synchrony is stable.

**4. Existence and stability of the traveling wave.** Next, we look at the existence and stability of the traveling wave,  $\theta(x, t) = \Omega t + x$ . Substituting  $\theta$  back into (2.4) gives us

$$(4.1) \quad \Omega = \omega + \frac{g_{syn}}{2\pi} \int_0^{2\pi} H_{syn}(y) dy + g_{gap} \int_0^{2\pi} J(y) H_{gap}(y) dy.$$

W.l.o.g., we can assume that the average of  $H_{syn}(y)$  is zero and so let  $I = \int_0^{2\pi} J(y) H_{gap}(y) dy$ ; (4.1) reduces to  $\Omega = \omega + g_{gap} I$ . (The value of the frequency is irrelevant to the stability calculation since the right-hand sides always involve terms of the form  $\theta(x, t) - \theta(y, t)$  so that adding  $Ct$  to  $\theta$ , where  $C$  is any constant, has no effect.) We prove the following theorem about the stability of the traveling wave.

**THEOREM 4.1.** *The traveling wave solution,  $\theta(x, t) = \Omega t + x$ , is a stable solution to (2.4) if we have*

$$\begin{aligned}
 Re(\lambda_n) &= -\frac{1}{2} g_{syn} n b_n + 2\pi g_{gap} \sum_{m=-\infty}^{-n-1} \frac{m}{4} [(c_m f_{n+m} - d_m e_{n+m}) - (c_m f_m - d_m e_m)] \\
 &\quad - 2\pi g_{gap} \sum_{m=-n}^{-1} \frac{m}{4} [(c_m f_{n+m} + d_m e_{n+m}) + (c_m f_m - d_m e_m)] \\
 &\quad - 2\pi g_{gap} \sum_{m=1}^{\infty} \frac{m}{4} [(c_m f_{n+m} - d_m e_{n+m}) - (c_m f_m - d_m e_m)] \\
 &\leq 0
 \end{aligned}$$

for  $n > 0$ , where

$$H_{syn}(y) = \sum_{n=0}^{\infty} a_n \cos ny + b_n \sin ny,$$

$$H_{gap}(y) = \sum_{n=0}^{\infty} c_n \cos ny + d_n \sin ny,$$

$$J(y) = \sum_{n=0}^{\infty} e_n \cos ny + f_n \sin ny.$$

*Proof.* Letting  $\theta(x, t) = \Omega t + x + \psi(x, t)$ , we write

$$(4.2) \quad \begin{aligned} \frac{\partial \psi}{\partial t} = & \frac{g_{syn}}{2\pi} \int_0^{2\pi} H'_{syn}(y) [\psi(x+y) - \psi(x)] dy \\ & + g_{gap} \int_0^{2\pi} J(-y) H'_{gap}(y) [\psi(x+y) - \psi(x)] dy + O(|\psi|^2). \end{aligned}$$

$\psi(x, t) = e^{inx} e^{\lambda_n t}$  solves (4.2) up to linear order. We solve for  $\lambda_n$  to get

$$(4.3) \quad \lambda_n = \frac{g_{syn}}{2\pi} \int_0^{2\pi} H'_{syn}(y) [e^{iny} - 1] dy + g_{gap} \int_0^{2\pi} J(-y) H'_{gap}(y) [e^{iny} - 1] dy.$$

We look at the real part of  $\lambda_n$ , for  $H_{syn}$ ,  $H_{gap}$ , and  $J$  real-valued,

$$Re(\lambda_n) = \frac{g_{syn}}{2\pi} \int_0^{2\pi} H'_{syn}(y) [\cos ny - 1] dy + g_{gap} \int_0^{2\pi} J(-y) H'_{gap}(y) [\cos ny - 1] dy.$$

When  $n = 0$ ,  $Re(\lambda_0) = 0$ , which corresponds to translation invariance. We need  $Re(\lambda_n) \leq 0$  for  $n \neq 0$ . Also, we want to make our analysis as general as possible. For this reason we use the complex Fourier series expansion for  $H_{syn}$ ,  $H_{gap}$ , and  $J$ . Let  $J(y) = \sum_{k=-\infty}^{\infty} \alpha_k e^{iky}$ ,  $H_{syn}(y) = \sum_{l=-\infty}^{\infty} \beta_l e^{ily}$ ,  $H_{gap}(y) = \sum_{m=-\infty}^{\infty} \gamma_m e^{imy}$ , where  $\alpha_{-k} = \alpha_k$ ,  $\beta_{-l} = \beta_l$ , and  $\gamma_{-m} = \gamma_m$ . Substituting these into (4.3) gives

$$\lambda_n = -ig_{syn} n \beta_{-n} + 2\pi i g_{gap} \sum_{m=-\infty}^{\infty} [m \gamma_m (\alpha_{-(n+m)} - \alpha_{-m})].$$

If we look at the real part of  $\lambda_n$ , we see that

$$\begin{aligned} Re(\lambda_n) = & -\frac{1}{2} g_{syn} n b_n + 2\pi g_{gap} \sum_{m=-\infty}^{-n-1} \frac{m}{4} [(c_m f_{n+m} - d_m e_{n+m}) - (c_m f_m - d_m e_m)] \\ & - 2\pi g_{gap} \sum_{m=-n}^{-1} \frac{m}{4} [(c_m f_{n+m} + d_m e_{n+m}) + (c_m f_m - d_m e_m)] \\ & - 2\pi g_{gap} \sum_{m=1}^{\infty} \frac{m}{4} [(c_m f_{n+m} - d_m e_{n+m}) - (c_m f_m - d_m e_m)], \end{aligned}$$

where  $H_{syn}$ ,  $H_{gap}$ , and  $J$  are given with the Fourier expansion with coefficients  $a_0 = 2\beta_0$ ,  $c_0 = 2\gamma_0$ ,  $e_0 = 2\alpha_0$ ,  $a_n = \beta_n + \beta_{-n}$ ,  $b_n = i(\beta_n - \beta_{-n})$ ,  $c_n = \gamma_n + \gamma_{-n}$ ,  $d_n = i(\gamma_n - \gamma_{-n})$ ,  $e_n = \alpha_n + \alpha_{-n}$ , and  $e_n = i(\alpha_n - \alpha_{-n})$ .  $\square$

In our case, the traveling wave is always stable. Substituting our parameters into the eigenvalue equation, we see that  $Re(\lambda_n) \leq -50g_{syn} - 824.27g_{gap} \leq 0$  for all positive values of  $g_{syn}$  and  $g_{gap}$ .

We close this section with some comments on the existence and stability of traveling waves in the discrete system for local gap junction coupling. Consider a discrete ring,

$$\frac{d\theta_j}{dt} = \omega + \sum_{i=-m}^m a_i H(\theta_{j+m} - \theta_j),$$

where  $m \ll N$  and  $N$  is the number of oscillators. The coupling constants  $a_i$  are nonnegative. Suppose that  $H$  is  $2\pi$ -periodic and that  $H'(x) > 0$  for  $-r < x < r$  and  $r > 0$ . Then, it follows from [7] that the synchronous state is asymptotically stable. Now, consider a traveling wave:

$$\theta_j = \Omega t + 2\pi j/N.$$

This satisfies the discrete model if and only if

$$\Omega = \omega + \sum_{i=-m}^m a_i H(2\pi i/N).$$

If  $m/N$  is sufficiently small, then

$$H'(\pm 2\pi m/M) > 0$$

since  $H'(x)$  is positive in some neighborhood of 0. Thus, again from [7], the traveling wave is asymptotically stable. Figure 2.1(b) shows that  $H'_{gap}(x) > 0$  over more than half the cycle surrounding the origin. Thus, we can pick  $m$  as large as  $N/4$  and still be assured that the traveling wave is stable. This shows that there is bistability between traveling waves and synchrony in the discrete model with small enough synaptic coupling.

**5. Numerical results.** In this section we (i) show that the bifurcation theory developed for the continuum model appears to hold for the discrete model by numerically simulating the latter, (ii) numerically extend the local bifurcation analysis to get the full picture for the discrete phase-model, (iii) numerically simulate the conductance-based model and show patterns similar to those found via our analysis, and (iv) compute the bifurcation diagram for a line of 20 oscillators which are *not* connected in a ring.

Figure 5.1 depicts the steady-state relative phases for a ring of 20 phase-oscillators using the interaction functions shown in Figure 2.1. The strength of the gap junction coupling is fixed at .01, and  $g_{syn}$  is varied along the vertical axis. Simulations are done by starting the relative phases close to synchrony and then letting them evolve until a steady state is reached. Figure 5.1(a) shows this steady state (color-coded) for each value of  $g_{syn}$  examined. (We remark that in the phase model, the absolute value of the coupling parameters is irrelevant, and only their ratio matters.) Figure 5.1(b) shows vertical cross sections from part (a) to more clearly illustrate different types of solutions observed for various  $\rho \equiv g_{syn}/g_{gap}$  values. For example, when  $\rho = 0.3$ , there is no difference in phases of the oscillators, indicating that the system is synchronized. In contrast, between  $\rho \approx 0.35$  and  $\rho \approx 0.87$ , the solution is the

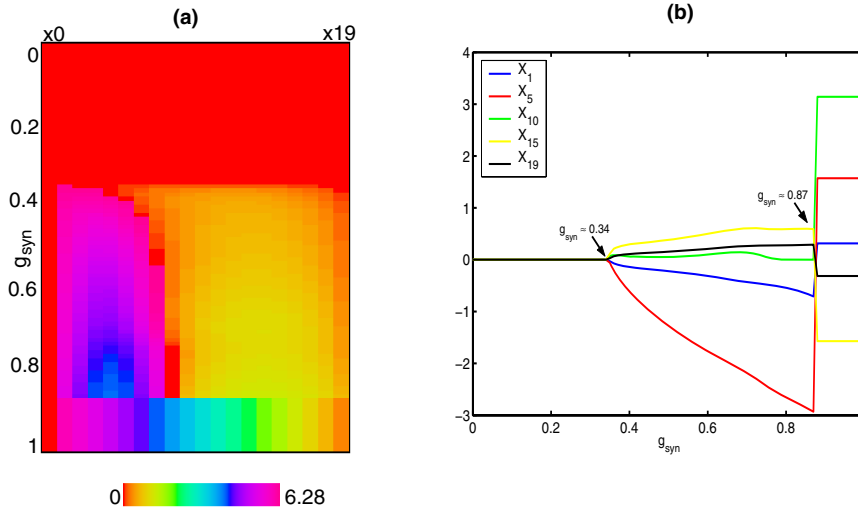


FIG. 5.1. Transition from synchrony to intermediate state and then to traveling wave. (a) illustrates an array plot of the relative phases of the oscillators as  $\rho \equiv g_{syn}/g_{gap}$  is increased; (b) shows the phases of some oscillators as  $\rho$  is increased.

patterned state which bifurcates from the synchronous state as described in section 3. As  $\rho$  increases beyond 0.87, the patterned state (which qualitatively resembles a cosine wave) disappears and leaves a traveling wave as the only solution. The traveling wave is, in fact, stable for all  $\rho$  shown in the diagram, so that for  $\rho < 0.87$  there is bistability. The loss of stability of the synchronous state occurs at  $\rho \approx 0.35$ , which is very close to the value of 0.3476 predicted in section 2.

To give the reader some intuition for the patterns, we depict the spatio-temporal patterns in terms of their absolute phase in Figure 5.2. As we increase the relative coupling strength, we see the transition from synchrony to a stable patterned state (compare 5.2(a) and (b)). This is the state which arises via the pitchfork bifurcation calculated in section 2. As we further increase  $g_{syn}$ , the patterned state disappears and produces traveling waves; the transition from the patterned state to the waves is shown in Figure 5.2(c). Finally, for larger  $g_{syn}$ , only the traveling wave remains.

The analytic calculations along with the numerical calculations of the phase reduced model show that as the inhibition increases, the synchronous state loses stability to a patterned state in which the relative phases are close to a cosine wave. Further increases in the inhibition result in a deepening of this pattern, followed by a transition to a traveling wave. In Figure 5.3, we show the result of a simulation of the biophysical model as the synaptic inhibition increases. To match the theory, we have made the connections periodic, so that the last cell is coupled to the first. Figure 5.3(a) shows a clear phase pattern in which the oscillators at the end lag the ones in the middle. This corresponds to the patterned state shown in Figures 5.2(b) and 5.1(a), when  $\rho \approx 0.4$ . For a larger amount of inhibition, the behavior becomes quite complicated and, after a long transient, begins a transition to traveling waves, as shown in Figure 5.3(b). Thus, the phase model provides a very good description of the full biophysical model and has the advantage of being simple enough to analyze.

We conclude this section with some comments on the simplification to a ring of oscillators instead of a line as in the original model. The main reason for assuming a

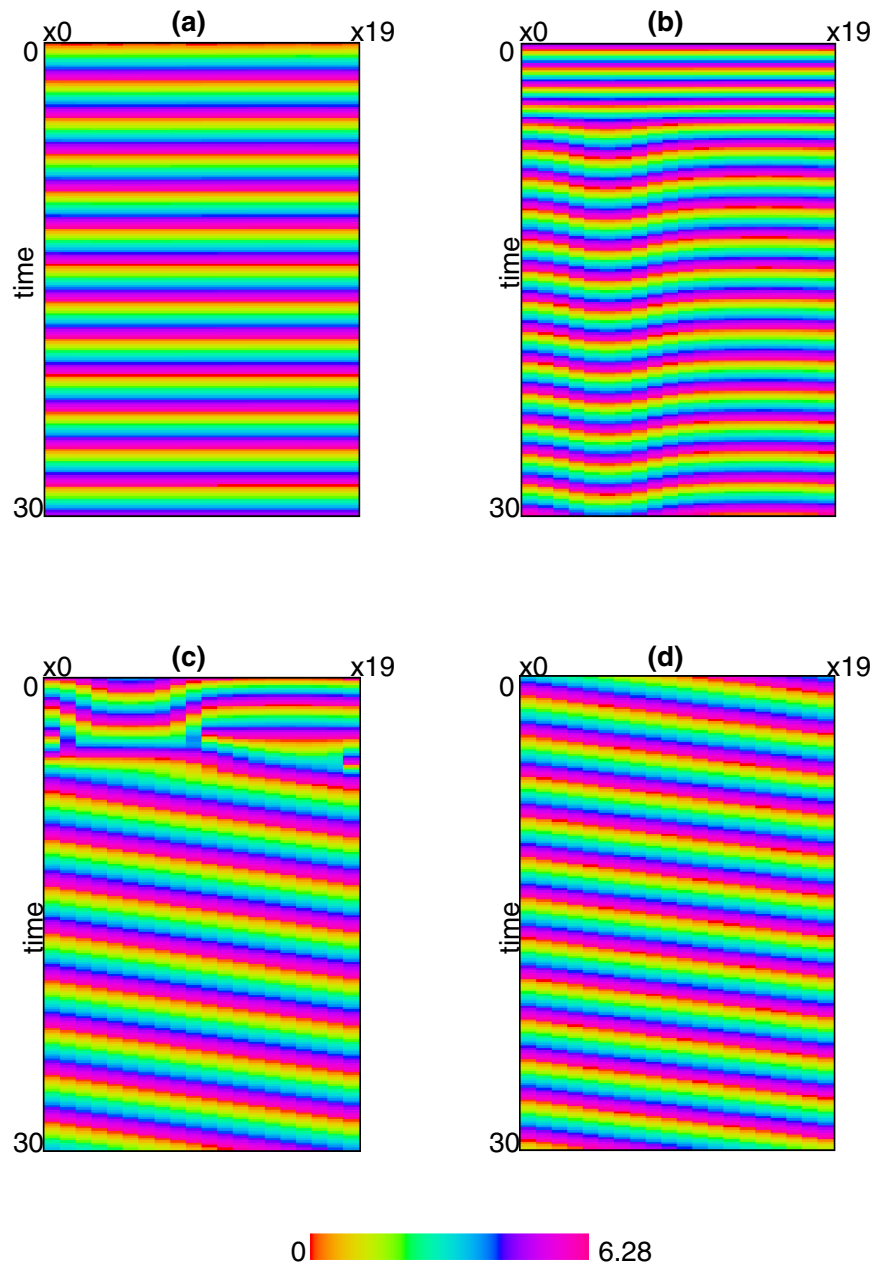


FIG. 5.2. Evolution of the solution to the discrete phase model is shown as we change  $g_{syn}$  while  $g_{gap}$  is kept at the value 0.03. (a) shows synchronous solution when  $g_{syn} = 0.01$ , (b) shows the intermediate state when  $g_{syn} = 0.02$ , (c) shows the transition to the traveling wave solution when  $g_{syn} = 0.03$ , and (d) shows the traveling wave solution when  $g_{syn} = 0.04$ .

ring is that the analytic calculations are then possible. If, instead of a ring, we consider a line of oscillators and choose the coupling functions so that the synchronous state exists, we can explore the stability and bifurcations as the antisynchronous (synaptic inhibition) coupling increases. Rather than attempt these calculations analytically, we instead display numerical simulations for the phase model with all-to-all synaptic

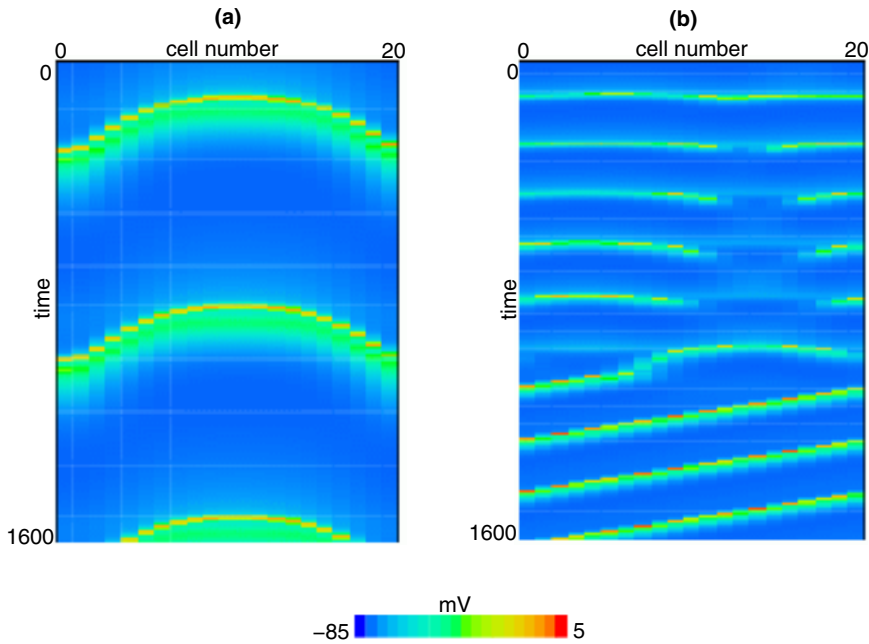


FIG. 5.3. Behavior of the conductance-based model for  $g_{syn} = 0.03$  and  $g_{gap} = 0.07$ . Voltage is plotted for each oscillator.

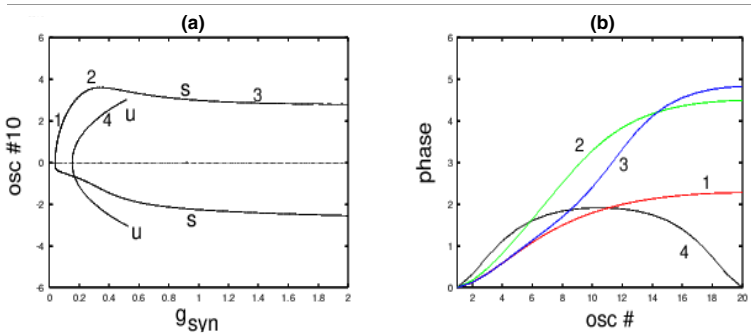


FIG. 5.4. Behavior of 20 phase oscillators in a line as the synaptic coupling increases. (a) The relative phase of oscillator 10;  $g_{gap} = 1$  and the interaction functions are the same as in the ring model. (b) Spatial profiles with various solutions from (a).  $u$  refers to the solution being unstable, and  $s$  means the solution is stable.

coupling and nearest neighbor gap junction coupling.

Figure 5.4 shows the behavior for a line of 20 oscillators. By considering a linear array, the symmetry in the ring model was broken, and we are able to use the AUTO bifurcation package [5]. We depict two pitchfork bifurcations. The first emerges as a stable supercritical bifurcation. The pattern is like a half of a cosine wave, as opposed to the full cycle seen in a ring. The ring of oscillators can be imagined as a pair of lines joined symmetrically through the midline. Thus, we expect that the first bifurcation would be “half” of that seen in the ring (see curve 1 in Figure 5.4(b)). As  $g_{syn}$  increases, this branch seems to approach a solution which looks like a traveling

wave (Figure 5.4(b) curves 2 and 3). There is no true traveling wave in the line due to the boundary conditions; however, the solutions in the figure look like traveling waves. A second branch bifurcates supercritically but it inherits the instability of the synchronous branch, so that it is unstable. The shape of this solution is shown by curve 4 in Figure 5.4(b). As these solutions were unstable, they were not continued beyond  $g_{syn} = 0.5$ . Thus, while the details are somewhat different, the ultimate result is the same for both a ring and a linear array: as  $g_{syn}$  increases, synchrony loses stability, and for large enough  $g_{syn}$  there is a traveling wave. The traveling wave exists for all values of  $g_{syn}$  in the ring model but not for the linear array.

**6. Discussion.** In this paper, we have shown that the combination of long range inhibitory synaptic coupling with local gap junction coupling was sufficient to induce a destabilization of the synchronous state. A new state which is not a traveling wave but rather a spatially organized phase shift stably appears and is lost as the amount of long range inhibitory coupling increases. Numerical solutions indicate that the only remaining attracting state is a traveling wave. Our mathematical results concern a network on a ring; the original motivation for this problem is the slug olfactory lobe, which is actually a line of oscillators. However, it is known from our earlier work [14] that boundary effects are enough to induce patterns of phases that depend very strongly on the choices of boundary conditions at the edges. To avoid this difficulty, we have considered periodic boundary conditions which eliminate questions about the behavior at the edges. In spite of this simplifying assumption, we see that the linear array and the ring behave similarly, at least when the inhibition is sufficiently large compared to electrical coupling.

A number of studies have investigated interactions between electrical coupling and synaptic coupling between neural oscillators. This problem is important since inhibitory interneurons in the mammalian neocortex appear to be coupled with both types of interactions. These networks may act as the “pacemakers” for 40 Hz oscillations observed in the cortex during various cognitive tasks [20]. Most theoretical explorations involve either pairs of cells or globally coupled networks. In most instances, both the synaptic and the electrical coupling encourage synchrony, so that there is not a chance for pattern formation. However, [4] has shown that gap junctions can either stabilize or destabilize synchrony, depending on the shape of the action potential, while [17] has shown that the intrinsic currents also affect whether or not electrical coupling is synchronizing. Combining coupling that destabilizes with coupling that stabilizes synchrony can be expected to produce other patterns of activity besides waves. Such patterns may play some role in cortical processing of information and may confer certain computational advantages [8].

**Appendix A.** To calculate the normal form for the bifurcation, we match the “ $\epsilon$ ” terms from (3.6):

$$\Omega_1 = \int_0^{2\pi} A_1(y') [\psi_1(x - y') - \psi_1(x)] dy' \equiv \mathcal{L} \psi_1.$$

We integrate both sides of the equation with respect to  $x$  to get  $\Omega_1 = 0$ . If we solve  $\mathcal{L}\psi_1 = 0$ , we get that  $\psi_1(x) = ze^{ix} + \bar{z}e^{-ix}$  w.l.o.g. Next, we look at  $\epsilon^2$  terms:

$$\begin{aligned} \Omega_2 = \mathcal{L} \psi_2 + \int_0^{2\pi} A_2(y') [\psi_1(x - y') - \psi_1(x)]^2 dy' \\ + \frac{g_1 \alpha_1}{2\pi} \int_0^{2\pi} [\psi_1(x - y') - \psi_1(x)] dy'. \end{aligned} \tag{A.1}$$

Substituting  $\psi_1$  into (A.1) and integrating with respect to  $x$ ,

$$\int_0^{2\pi} \Omega_2 dx = 8\pi z \bar{z} [B_0(A_2) - B_1(A_2)],$$

$$\Omega_2 = 4z \bar{z} [B_0(A_2) - B_1(A_2)],$$

where  $B_n(A_j) = \int_0^{2\pi} A_j(y') e^{\pm iny'} dy'$ ,  $j = 1, 2, 3$ . Now, we multiply (A.1) by  $e^{-ix}$ ,

$$0 = -2\pi g_1 \alpha_1 z,$$

which implies  $g_1 = 0$ . So, we can write  $g_{syn} = g_{syn}^* + \epsilon^2 g_2$ , and we solve for  $\psi_2$ :

$$(A.2) \quad 0 = \mathcal{L} \psi_2 + (z^2 e^{2ix} + \bar{z}^2 e^{-2ix}) [B_2(A_2) + B_0(A_2) - 2B_1(A_2)].$$

We now propose that  $\psi_2 = C z^2 e^{2ix} + \bar{C} \bar{z}^2 e^{-2ix}$  and substitute back into (A.1) to get

$$0 = [B_2(A_1) - B_0(A_1)] (C z^2 e^{2ix} + \bar{C} \bar{z}^2 e^{-2ix}) + [B(A_2) + B_0(A_2) - 2B_1(A_2)] (z^2 e^{2ix} + \bar{z}^2 e^{-2ix}).$$

Looking at the coefficients of the  $z^2$  term gives

$$(A.3) \quad C = \frac{2B_1(A_2) - B_2(A_2) - B_0(A_2)}{B_2(A_1) - B_0(A_1)}.$$

We have to make sure here that the denominator is nonzero. This is easy to see, since  $B_2(A_1) - B_0(A_1) = 0$  would imply that  $g_{syn}^* = \frac{gs\beta_1(I_2-1)}{\alpha_2}$ , which is not true since  $g_{syn}^* = \frac{g_{gap}\beta_1(I_1-1)}{\alpha_2}$  and  $I_1 > I_2$ .

Next, we look at  $\epsilon^3$  terms:

$$(A.4) \quad \begin{aligned} \Omega_3 = \mathcal{L} \psi_3 + \int_0^{2\pi} A_3(y') [\psi_1(x - y') - \psi_1(x)]^3 dy' \\ + 2 \int_0^{2\pi} A_2(y') [\psi_1(x - y')\psi_2(x - y') + \psi_1(x)\psi_2(x)] dy' \\ - 2 \int_0^{2\pi} A_2(y') [\psi_1(x - y')\psi_2(x) + \psi_1(x)\psi_2(x - y')] dy' \\ + \frac{g_2\alpha_1}{2\pi} \int_0^{2\pi} [\psi_1(x - y') - \psi_1(x)] dy'. \end{aligned}$$

Let us look at the terms in (A.4) closely:

$$\begin{aligned} [\psi_1(x - y') - \psi_1(x)]^3 &= [ze^{ix}e^{-iy'} + \bar{z}e^{-ix}e^{iy'} - ze^{ix} - \bar{z}e^{-ix}]^3 \\ &= z^3 e^{3ix} e^{-3iy'} + 3z^2 \bar{z} e^{ix} e^{-iy'} + 3z \bar{z}^2 e^{-ix} e^{iy'} + \bar{z}^3 e^{-3ix} e^{3iy'} \\ &\quad - 3z^3 e^{3ix} e^{-2iy'} - 3z^2 \bar{z} e^{ix} e^{-2iy'} - 6z^2 \bar{z} e^{ix} \\ &\quad - 6z \bar{z}^2 e^{-ix} - 3z \bar{z}^2 e^{-ix} e^{2iy'} - 3\bar{z}^3 e^{-3ix} e^{2iy'} \\ &\quad + 3z^3 e^{3ix} e^{iy'} + 3z^2 \bar{z} e^{ix} e^{iy'} + 6z^2 \bar{z} e^{ix} e^{-iy'} \\ &\quad + 6z \bar{z}^2 e^{-ix} e^{iy'} + 3z \bar{z}^2 e^{-ix} e^{-iy'} + 3\bar{z}^3 e^{-3ix} e^{iy'} \\ &\quad - z^3 e^{3ix} - 3z^2 \bar{z} e^{ix} - 3z \bar{z}^2 e^{-ix} - \bar{z}^3 e^{-3ix}. \end{aligned}$$

Let  $T = [\psi_1(x - y')\psi_2(x - y') + \psi_1(x)\psi_2(x) - \psi_1(x - y')\psi_2(x) - \psi_1(x)\psi_2(x - y')]$ ; then

$$\begin{aligned}
T &= (ze^{ix}e^{-iy'} + \bar{z}e^{-ix}e^{iy'}) (Cz^2e^{2ix}e^{-2iy'} + \bar{C}\bar{z}^2e^{-2ix}e^{2iy'}) \\
&\quad + (ze^{ix} + \bar{z}e^{-ix})(Cz^2e^{2ix} + \bar{C}\bar{z}^2e^{-2ix}) \\
&\quad - (ze^{ix}e^{-iy'} + \bar{z}e^{-ix}e^{iy'}) (Cz^2e^{2ix} + \bar{C}\bar{z}^2e^{-2ix}) \\
&\quad - (ze^{ix} + \bar{z}e^{-ix})(Cz^2e^{2ix}e^{-2iy'} + \bar{C}\bar{z}^2e^{-2ix}e^{2iy'}) \\
&= Cz^3e^{3ix}e^{-3iy'} + \bar{C}\bar{z}\bar{z}^2e^{-ix}e^{iy'} + Cz^2\bar{z}e^{ix}e^{-iy'} \\
&\quad + \bar{C}\bar{z}^3e^{-3ix}e^{3iy'} + Cz^3e^{3ix} + \bar{C}\bar{z}\bar{z}^2e^{-ix} \\
&\quad + Cz^2\bar{z}e^{ix} + \bar{C}\bar{z}^3e^{-3ix} - Cz^3e^{3ix}e^{-iy'} - \bar{C}\bar{z}\bar{z}^2e^{-ix}e^{-iy'} \\
&\quad - Cz^2\bar{z}e^{ix}e^{iy'} - \bar{C}\bar{z}^3e^{-3ix}e^{iy'} \\
&\quad - Cz^3e^{3ix}e^{-2iy'} - \bar{C}\bar{z}\bar{z}^2e^{-ix}e^{2iy'} \\
&\quad - Cz^2\bar{z}e^{ix}e^{-2iy'} - \bar{C}\bar{z}^3e^{-3ix}e^{2iy'}.
\end{aligned}$$

Substituting  $\psi_1$  and  $\psi_2$  into (A.4) and using the expansions for  $[\psi_1(x - y') - \psi_1(x)]^3$  and  $T$ , we then integrate with respect to  $x$  to get  $\Omega_3 = 0$ . Next, multiply both sides by  $e^{-ix}$  and integrate with respect to  $x$  to get

$$\begin{aligned}
0 &= z^2\bar{z} \int_0^{2\pi} A_3(y') [9e^{-iy'} + 3e^{iy'} - 3e^{-2iy'} - 9] dy' \\
&\quad + 2C z^2\bar{z} \int_0^{2\pi} A_2(y') [e^{-iy'} - e^{iy'} - e^{-2iy'} + 1] dy' - g_2\alpha_1 z.
\end{aligned}$$

We can simplify this as follows:

$$0 = z^2\bar{z}[12B_1(A_3) - 3B_2(A_3) - 9B_0(A_3) + 2C B_0(A_2) - 2CB_2(A_2)] - g_2\alpha_1 z.$$

By letting  $\zeta = 12B_1(A_3) - 3B_2(A_3) - 9B_0(A_3) + 2C B_0(A_2) - 2CB_2(A_2)$  and  $\eta = -g_2\alpha_1$ , we have the normal form at the bifurcation point as

$$0 = \zeta z^2\bar{z} + \eta z.$$

**Appendix B.** We use the biophysical model given in [6]. Each uncoupled bursting cell in the Limax model has the form

$$\begin{aligned}
C \frac{dV}{dt} &= -I_L - I_K - I_{Ca} \\
&= -g_L(V - E_L) - g_K n^4(V - E_K) - g_{Ca} m^2 h(V - E_{Ca}),
\end{aligned}$$

where  $n, h$  obey the equations

$$\begin{aligned}
\frac{dn}{dt} &= .075[a_n(V)(1 - n) - b_n(V)n], \\
\frac{dh}{dt} &= \frac{1.125(h_\infty(V) - h)}{\tau_h(V)},
\end{aligned}$$

with

$$\begin{aligned}
a_n(V) &= .032(-48 - V)/(\exp(-(48 + V)/5) - 1), \\
b_n(V) &= .5 \exp(-(43 + V)/40), \\
h_\infty(V) &= 1/(1 + \exp((V + 86)/4)), \\
\tau_h(V) &= \begin{cases} \text{if } (V < (-80)), \text{ then } (\exp((V + 470)/66.6)), \\ \text{else } (28 + \exp((V + 25)/-10.5)). \end{cases}
\end{aligned}$$

The activation gate for the T-type calcium current has the form

$$m(V) = 1/(1 + \exp(-(V + 60))).$$

The parameters are  $C = 2.66$ ,  $g_K = 5$ ,  $g_L = 0.024$ ,  $g_{Ca} = 2$ ,  $E_K = -90$ ,  $E_{Ca} = 140$ ,  $E_L = -82$ , and  $E_{syn} = -78$ . Using this model, we compute the approximations of the coupling functions as follows:

$$H_{syn}(x) = 35 + 200 \cos(x) + 32 \cos(2x) - 95 \sin(x) - 5 \sin(2x),$$

$$H_{gap}(x) = 87 - 50 \cos(x) - 37 \cos(2x) + 295 \sin(x) - 65 \sin(2x).$$

## REFERENCES

- [1] T. BEM, Y. LEFEUVRE, J. SIMMERS, AND P. MEYRAND, *Electrical coupling can prevent expression of adult-like properties in an embryonic neural circuit*, J. Neurophysiol., 87 (2002), pp. 538–547.
- [2] T. BEM AND J. RINZEL, *Short duty cycle destabilizes a half-center oscillator, but gap junctions restabilize the anti-phase pattern*, J. Neurophysiol., 91 (2004), pp. 693–703.
- [3] C. BOU-FLORES AND A. J. BERGER, *Gap junctions and inhibitory synapses modulate inspiratory motoneuron synchronization*, Neurophysiol., 85 (2001), pp. 1543–1551.
- [4] C. C. CHOW AND N. KOPELL, *Dynamics of spiking neurons with electrical coupling*, Neural Comp., 1 (1994), pp. 313–321.
- [5] B. ERMENTROUT, *Simulating, Analyzing, and Animating Dynamical Systems: A Guide to XPPAUT for Researchers and Students*, Software Environ. Tools 14, SIAM, Philadelphia, 2002.
- [6] B. ERMENTROUT, J. W. WANG, J. FLORES, AND A. GELPERIN, *Model for transition from waves to synchrony in the olfactory lobe of Limax*, J. Comput. Neurosci., 17 (2004), pp. 365–383.
- [7] G. B. ERMENTROUT, *Stable periodic solutions to discrete and continuum arrays of weakly coupled nonlinear oscillators*, SIAM J. Appl. Math., 52 (1992), pp. 1665–1687.
- [8] G. B. ERMENTROUT AND D. KLEINFELD, *Travelling electrical waves in cortex: Insight from phase dynamics and speculation on a computational role*, Neuron, 29 (2001), pp. 33–44.
- [9] G. B. ERMENTROUT AND N. KOPELL, *Multiple pulse interactions and averaging in systems of coupled neural oscillators*, J. Math. Biol., 29 (1991), pp. 195–217.
- [10] G. B. ERMENTROUT AND N. KOPELL, *Inhibition-produced patterning in chains of coupled nonlinear oscillators*, SIAM J. Appl. Math., 54 (1994), pp. 478–507.
- [11] M. GALARRETA AND S. HESTRIN, *A network of fast-spiking cells in the neocortex connected by electrical synapses*, Nature, 402 (1999), pp. 72–75.
- [12] N. KOPELL, *Toward a theory of modeling central pattern generators*, in Neural Control of Rhythmic Movements in Vertebrates, A. Cohen, ed., John Wiley, New York, 1988, pp. 396–413.
- [13] N. KOPELL AND B. ERMENTROUT, *Chemical and electrical synapses perform complementary roles in the synchronization of interneuronal networks*, Proc. Natl. Acad. Sci. USA, 101 (2004), pp. 15482–15487.
- [14] N. KOPELL AND G. B. ERMENTROUT, *Symmetry and phaselocking in chains of weakly coupled oscillators*, Comm. Pure Appl. Math., 39 (1986), pp. 623–660.
- [15] Y. KURAMOTO, *Chemical Oscillations, Waves and Turbulence*, Springer, New York, 1984.
- [16] T. J. LEWIS AND J. RINZEL, *Dynamics of spiking neurons connected by both inhibitory and electrical coupling*, J. Comput. Neurosci., 14 (2003), pp. 283–309.
- [17] B. PFEUTY, G. MATO, D. GOLOMB, AND D. HANSEL, *The combined effects of inhibitory and electrical synapses in synchrony*, Neural Comp., 17 (2005), pp. 633–670.
- [18] R. D. TRAUB, *Model of synchronized population bursts in electrically coupled interneurons containing active dendrites*, J. Comput. Neurosci., 2 (1995), pp. 283–289.
- [19] C. VAN VREESWIJK, L. F. ABBOTT, AND G. B. ERMENTROUT, *When inhibition not excitation synchronizes neural firing*, J. Comput. Neurosci., 1 (1994), pp. 313–321.
- [20] M. A. WHITTINGTON, R. D. TRAUB, N. KOPELL, B. ERMENTROUT, AND E. H. BUHL, *Inhibition based rhythms: Experimental and mathematical observations on network dynamics*, Int. J. Psychophysiol., 38 (2000), pp. 315–336.
- [21] A. T. WINFREE, *Biological rhythms and the behavior of populations of coupled oscillators*, J. Theor. Biol., 16 (1967), pp. 15–42.